Cell Reports, Volume *21*

Supplemental Information

Spatiotemporal Proteomic Profiling of Huntington's Disease Inclusions Reveals Widespread Loss of Protein Function

Fabian Hosp, Sara Gutiérrez-Ángel, Martin H. Schaefer, Jürgen Cox, Felix Meissner, Mark S. Hipp, F.-Ulrich Hartl, Rüdiger Klein, Irina Dudanova, and Matthias Mann

Hosp et al., *Figure S1*

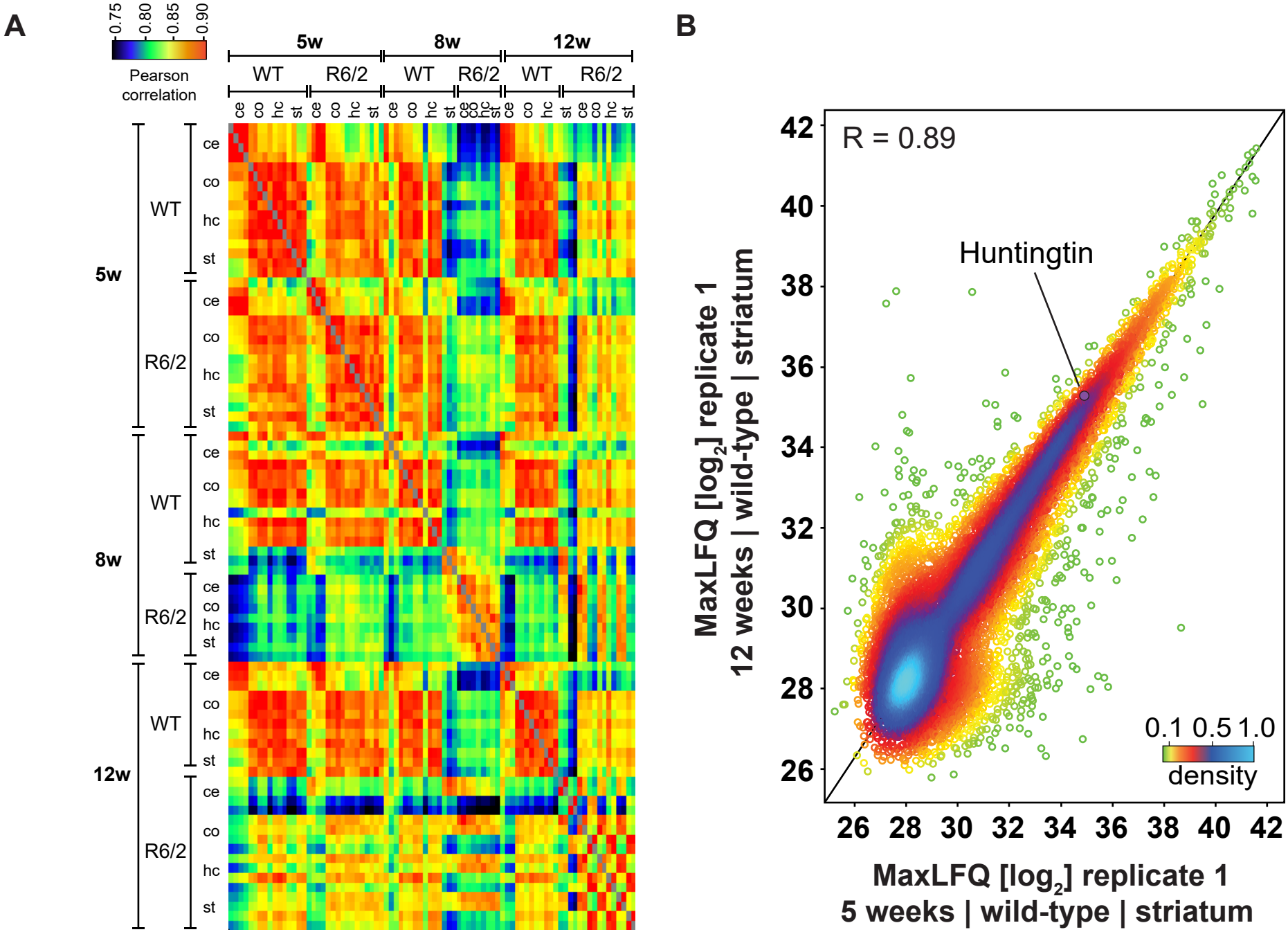

Figure S1. Reproducibility of total proteome measurements. Related to Figure 2. (A) The Pearson correlation of soluble proteomes of both R6/2 and wild-type (WT) mice for all brain regions across time is plotted as heatmap visualization. **(B)** Scatterplot of normalized label-free intensity for proteins quantified in the soluble striatal proteome of 5- or 12-week-old WT mice reveals only few changes in the brain proteome between these two age groups; Pearson correlation is indicated; data points colored by local point density.

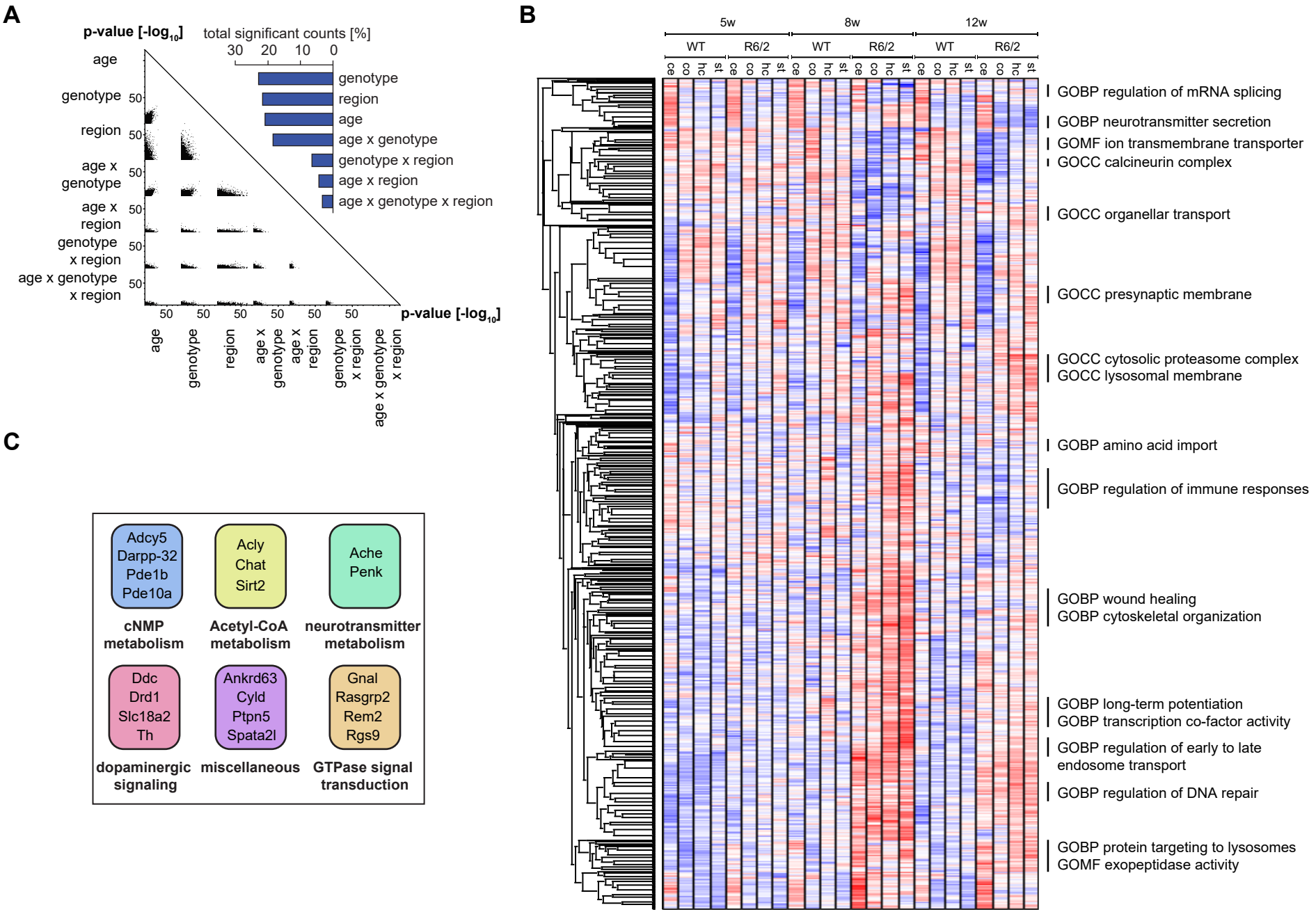

Figure S2. Loss of MSN-specific proteins. Related to Figure 3. (A) Differentially expressed proteins were identified by three-way ANOVA. Each dot represents a protein that the ANOVA finds significantly regulated for the indicated variables and combinations thereof. **(B)** Annotation matrix of protein attributes, such as complexes, gene ontologies and pathways highlights changes in the spatiotemporal composition of the soluble fraction; color code indicates the normalized median abundance of the proteins belonging to each category relative to the overall distribution of all proteins; selected annotations are highlighted; red most abundant, blue least abundant; Mann-Whitney U test (BH-FDR<0.05). **(C)** Grouping of top 20 candidates most similar to the Pde10a expression profile by protein function.

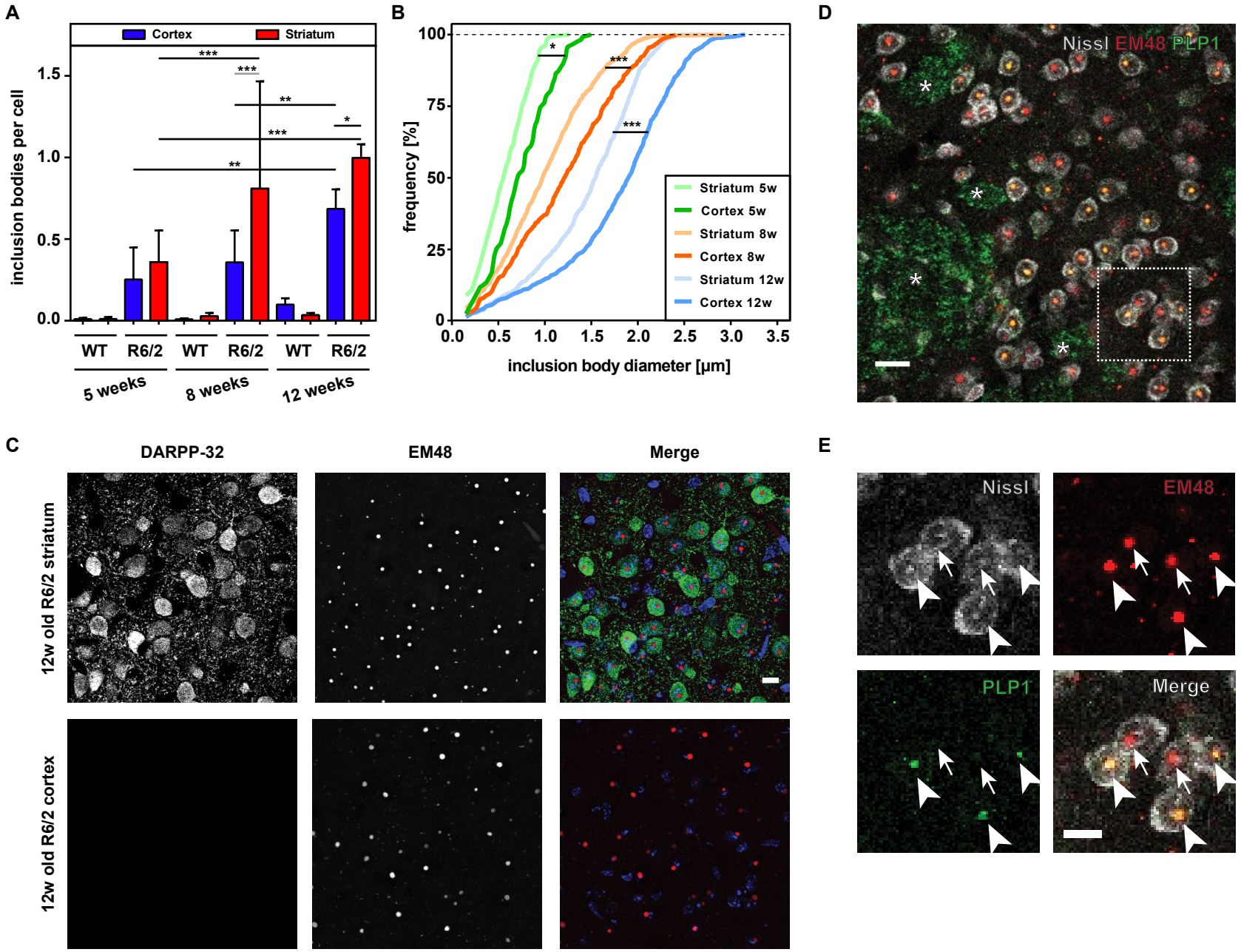

Figure S3. Quantification of HTT IBs from cortical and striatal tissue of R6/2 mice. Related to Figure 5. (A) Immunohistochemistry-based counting of inclusions from 5, 8 or 12-week-old R6/2 and WT mice; one-way ANOVA with Bonferroni's multiple comparison test, * $p<0.05$, ** $p<0.01$, *** $p<0.001$; n=3. **(B)** Frequency distribution of the data in Fig. S3A; one-way ANOVA with Bonferroni's multiple comparison test, * $p<0.05$, ** $p<0.01$, *** $p<0.001$; n=3. **(C)** Immunohistochemistry staining of cortical and striatal tissue of R6/2 mice; DAPI, blue; DARPP-32 for medium spiny neuron staining, green; EM48 for HTT inclusion staining, red; scale bar is 10 µm. **(D)** Representative single-plane immunofluorescence in a 12-week-old R6/2 striatum showing colocalization of PLP1 protein with IBs; Nissl staining for neurons, grey; EM48 staining for HTT IBs, red; PLP1 staining, green; asterisks mark white matter bundles of the striatum; scale bar is 20 µm. **(E)** Close-up of the colocalization; arrowheads point to PLP1 sequestered in IBs; arrows point to IBs without colocalization; scale bar is 10 µm.

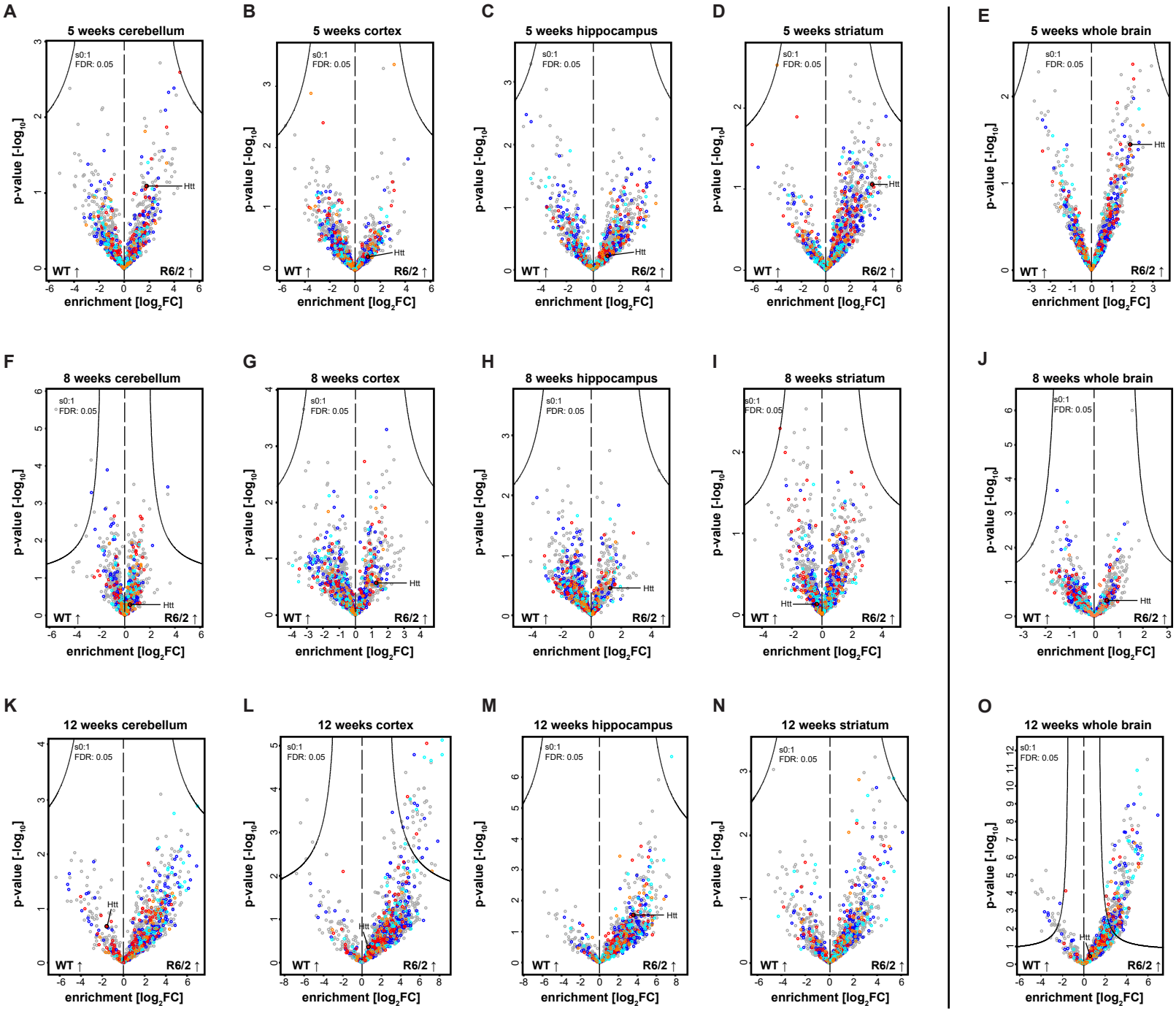

Figure S4. Volcano plots of insoluble fractions. Related to Figure 5. (A-D) Enrichment of proteins in the insoluble fractions is plotted by Volcano plots of all brain regions for 5 weeks, **(E)** 5 weeks whole brain, **(F-I)** all brain regions for 8 weeks, **(J)** 8 weeks whole brain, **(K-N)** all brain regions for 12 weeks and **(O)** 12 weeks whole brain. Color coding as in Figure 5C.

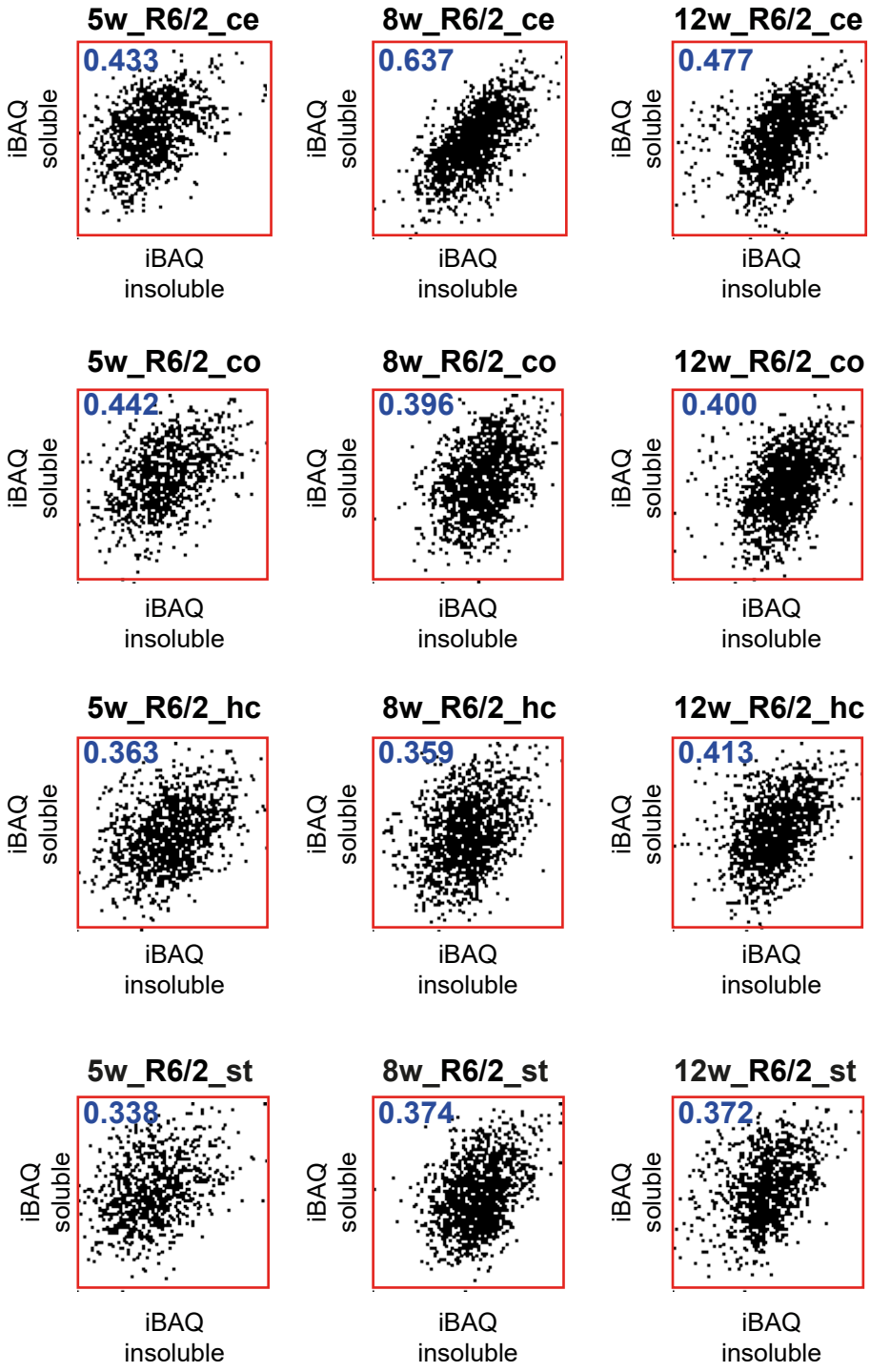

Figure S5. Correlation of protein abundance. Related to Figure 5. Correlation of iBAQ copy numbers for both soluble and insoluble proteins from R6/2 mice across all brain regions and time points. Pearson correlation is indicated.

Hosp et al., *Figure S6*

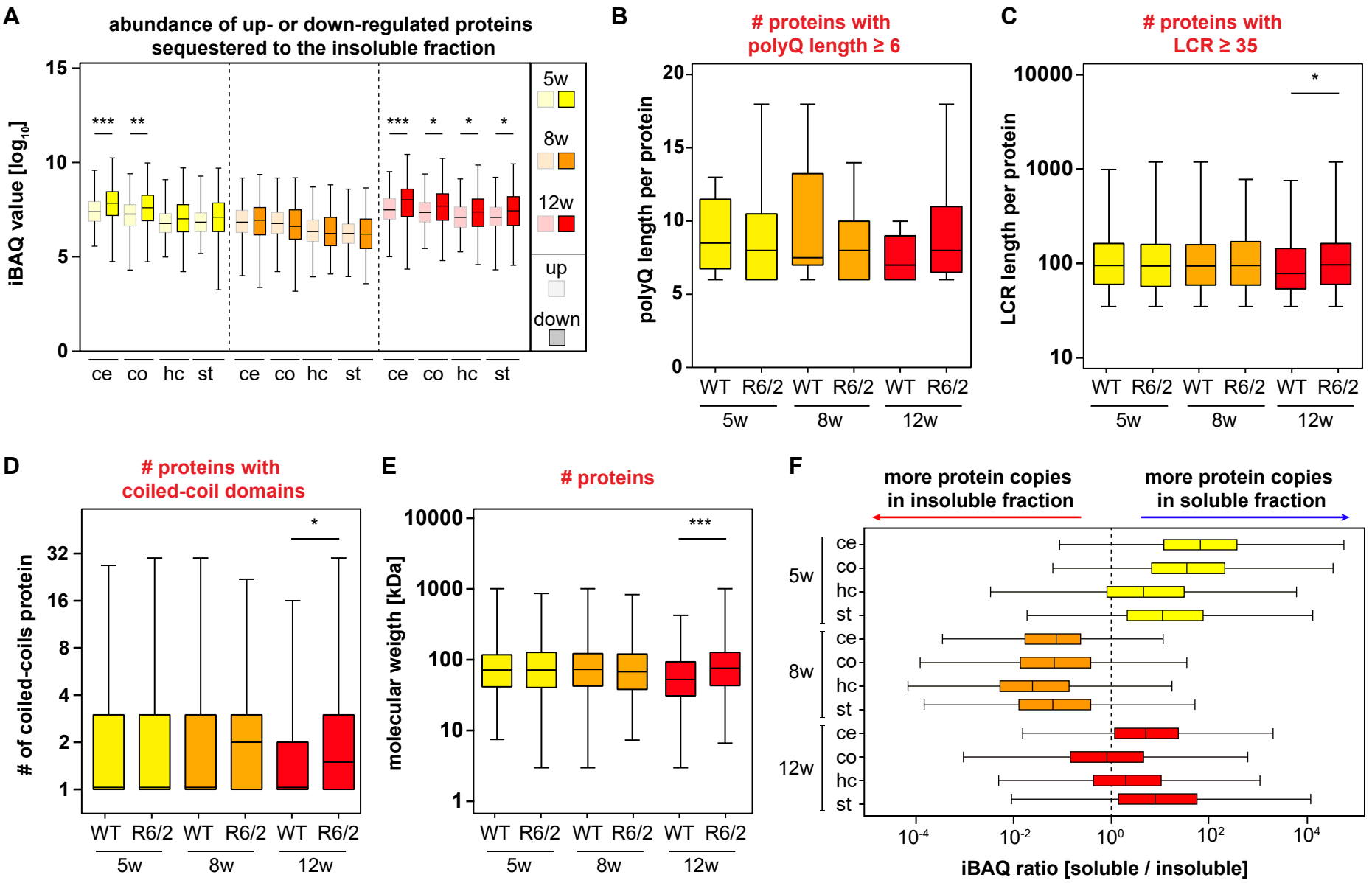

Figure S6. Degree of protein sequestration. Related to Figure 5. (A) Boxplot of iBAQ values for the most up- or down-regulated proteins in the soluble proteome (clusters 1-4, Figure 3C) being sequestered to the insoluble fraction; one-way ANOVA with Bonferroni's multiple comparison test, * $p<0.05$, ** $p<0.01$, *** $p<0.001$; n=3. **(B-E)** Sequence motif analyses across time; two-sided Mann-Whitney U test, * $p<0.05$, *** $p<0.001$. **(F)** Boxplots of all brain regions over time displaying the iBAQ ratio of proteins in the soluble over the insoluble fraction.

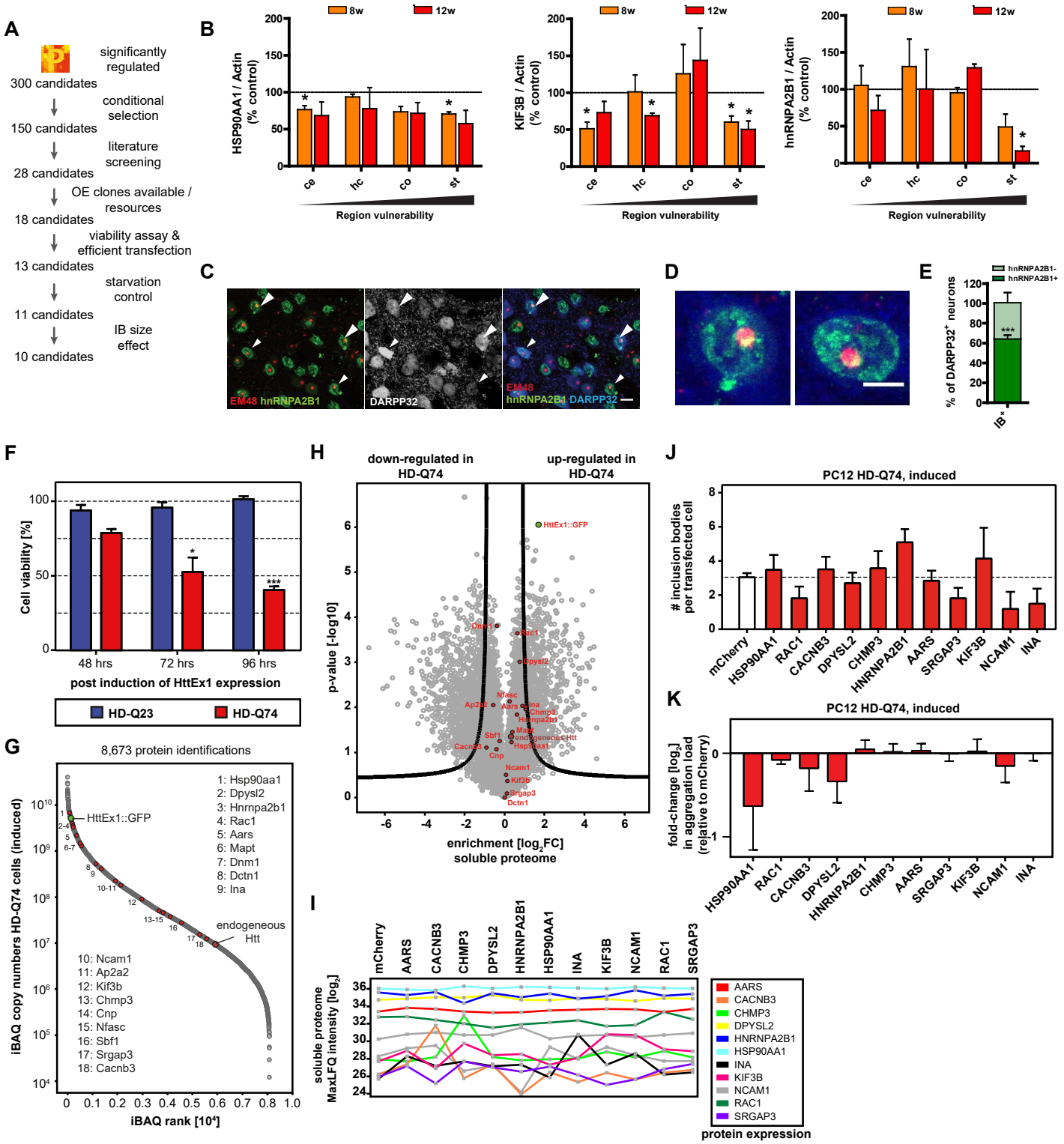

Figure S7. Validation of candidates from the proteomic screen. Related to Figure 7. (A) Candidate selection. **(B)** Quantification of candidates in immunoblots of brain regions from 8- and 12-week-old R6/2 mice, normalized to WT controls (dotted line); Student's t-test, *p<0.05; n=3-4. Striatal data is also shown in Figure 7. **(C)** Representative single-plane images of 12-week-old R6/2 striatum with nuclear hnRNPA2B1 accumulations; EM48 staining for HTT inclusion bodies, red; hnRNPA2B1, green; DARPP-32 staining for MSNs, blue; arrowheads, DARPP32+ neurons containing IBs and showing a nuclear accumulation of hnRNPA2/B1; scale bar is 10 µm. **(D)** Examples of two DARPP32+ neurons showing colocalization (yellow) of hnRNPA2B1 with the IB; scale bar is 5 µm. **(E)** Quantification of nuclear accumulation of hnRNPA2/B1 in DARPP32+ neurons with IB, in the striatum of 12-week-old R6/2 mice; there were significantly more neurons with than without hnRNPA2B1accumulation, Student's t-test, ** p<0.001; n=3 mice; 7 image fields each. In all neurons with hnRNPA2B1 accumulation, which represent 62% of all DARPP32+ cells, some degree of colocalization was always observed between the IB and hnRNPA2B1, as shown in (D). **(F)** Induction of HttEx1 expression in PC12 cells leads to polyQ length-dependent cell death; multiple t-test (two-tailed) with Benjamini-Hochberg correction; *FDR<0.05, ***FDR<0.001; n=3. **(G)** Ranking of HD-Q74 proteins by iBAQ copy numbers, selected candidates are indicated in red. **(H)** Changes in the proteome of HD-Q74 between induced and non-induced cells. **(I)** Soluble protein levels in HD-Q74 cells transfected with the different candidates. **(J)** Number of IBs per cell in HD-Q74 cells transfected with the candidates; multiple two-tailed t-test with Benjamini-Hochberg correction; *FDR<0.05; n=3. **(K)** Log2FC in aggregation load as determined by quantification of slot blot assays of HD-Q74 cell lysates transfected with the candidates, anti-GFP staining; multiple two-tailed t-test with Benjamini-Hochberg correction; *FDR<0.05; normalized to mCherry transfection controls; n=3.

Supplemental Experimental Procedures

RESOURCE TABLE

REAGENT or RESOURCE	SOURCE	IDENTIFIER
Antibodies		
Rabbit monoclonal anti-myc	Cell Signaling	Cat# 2278
Rabbit polyclonal anti-myc	Sigma-Aldrich	Cat# C3956
Rabbit monoclonal anti-flag	Sigma-Aldrich	Cat# F7425
Rat monoclonal anti-HA	Sigma-Aldrich	Cat# 11867423001
Rabbit polyclonal anti-HA	Sigma-Aldrich	Cat# H6908
Rat monoclonal anti-GFP	Chromotek	Cat# 3h9
Rabbit monoclonal anti-GAPDH	Cell Signaling	Cat# 2118
Mouse monoclonal anti-Huntingtin	Milipore	Cat# MAB5374
Rabbit monoclonal anti-DARPP-32	Abcam	Cat# ab40801
Mouse monoclonal anti-hnRNPA2B1	Santa Cruz Biotechnology, Inc.	Cat# sc-374053
Mouse monoclonal anti-KIF3B	Santa Cruz Biotechnology, Inc.	Cat# sc-514165
Rabbit polyclonal anti-HSP90	New England Biolabs GmbH	Cat# 4877
Mouse monoclonal anti-β-Actin	Sigma-Aldrich	Cat# A5316
Rabbit polyclonal anti-PLP1	Abcam	Cat# ab28486
NeuroTrace 640/660 Nissl Stain	Thermo Fisher Scientific	Cat# N21483
Donkey polyclonal anti-Rabbit Cy2-conjugate	Jackson ImmunoResearch	Cat# 711-545-152
Donkey polyclonal anti-Rabbit Cy3-conjugate	Jackson ImmunoResearch	Cat# 711-165-152
Donkey polyclonal anti-Mouse Cy3-conjugate	Jackson ImmunoResearch	Cat# 711-165-151
Anti-Rabbit IgG, HRP-linked	Cell Signaling	Cat# 7074
Chemicals, Peptides, and Recombinant Proteins		
Benzonase	Sigma-Aldrich	Cat#E1014
Hygromycin B	Thermo Fisher Scientific	Cat#10687010
G418	Thermo Fisher Scientific	Cat#10131035
Doxycycline	Sigma-Aldrich	Cat#D9891

Lysyl Endopeptidase LysC	Wako Chemicals	Cat# 129-02541
Trypsin	Sigma-Aldrich	Cat# T6567
Lipofectamine LTX with Plus Reagent	Thermo Fisher Scientific	Cat# 15338100
ProLong Gold antifade reagent	Life Technologies	Cat# P36930
Critical Commercial Assays		
Pierce LDH Cytotoxicity Assay Kit	Thermo Fisher Scientific	Cat# 88953
Deposited Data		
Proteomic dataset	This study	ProteomeXchange PXD004973
Mouse UniprotKB/Swiss-Prot database (Mouse UniProt 2014-07)	N/A	http://www.uniprot.org/proteomes
Brain peptide library for MS matching	(Sharma et al., 2015)	N/A
Experimental Models: Cell Lines		
Rat pheochromocytoma PC12 HDExon1-Q23	Gift from David Rubensztein, (University of Cambridge, UK)	N/A
Rat pheochromocytoma PC12 HDExon1-Q74	Gift from David Rubensztein, (University of Cambridge, UK)	N/A
Experimental Models: Organisms/Strains		
R6/2 (B6CBA-Tg(HDexon1)62gpb/1J) female mice	The Jackson Laboratory	Stock No: 002810
Recombinant DNA		
Plasmid C-term Myc + DDK_AARS	BioCat	RC202136-OR
Plasmid C-term Myc + DDK_AP2A2	BioCat	RC203018-OR
Plasmid C-term Myc + DDK_CACNB3	BioCat	RC207229-OR
Plasmid C-term Myc + DDK_CHMP3	BioCat	RC220006-OR
Plasmid C-term Myc + DDK_CNP	BioCat	RC207038-OR
Plasmid C-term Myc + DDK_DCTN1	BioCat	RC211975-OR
Plasmid C-term Myc + DDK_DNM1	BioCat	RC206284-OR
Plasmid C-term Myc + DDK_DPYSL2	BioCat	RC231368-OR
Plasmid C-term Myc + DDK_HDGF	BioCat	RC204148-OR
Plasmid C-term Myc + DDK_HNRNPA2B1	BioCat	RC219318-OR
Plasmid N-term HA_HSP90AA1	Gift from William Sessa (Yale School of Medicine)	AddGene #22487 (Garcia-Cardena et al., 1998)
Plasmid C-term Myc + DDK_INA	BioCat	RC202877-OR

Plasmid C-term Myc + DDK_KIF3B	BioCat	RC213911-OR
Plasmid N-term mApple_MAPT	Gift from Michael Davidson (National High Magnetic Field Laboratory)	AddGene #54924
Plasmid C-term Myc + DDK_NCAM1	BioCat	RC207890-OR
Plasmid N-term HA_NFASC	Gift from Vann Bennett (Duke University School of Medicine)	AddGene #31061 (Zhang et al., 1998)
Plasmid N-term Myc_RAC1	Gift from Lawrence Kirschner (Ohio State University)	AddGene #37030 (Manchanda et al., 2013)
Plasmid C-term Myc + DDK_SBF1	BioCat	RC222090-OR
Plasmid C-term Myc + DDK_SRGAP3	BioCat	RC214288-OR
Plasmid mCherry	This study	N/A
Software and Algorithms		
MaxQuant version 1.5.1.1	(Cox and Mann, 2008)	http://www.biochem.mpg.de5111795/maxquant
Perseus version 1.5.2.11	(Tyanova et al., 2016b)	http://www.biochem.mpg.de/5111810/perseus
Coils	(Lupas et al., 1991)	N/A
ImageJ version 1.49i	NIH	N/A

CONTACT FOR REAGENT AND RESOURCE SHARING

Further information and requests for reagents may be directed to, and will be fulfilled by the corresponding authors Irina Dudanova (idudanova@neuro.mpg.de) or Matthias Mann (mmann@biochem.mpg.de).

METHOD DETAILS

CSF Extraction and Preparation of Mouse Brain Regions

Mice were euthanized by carbondioxide inhalation, then shaved between the shoulders and below the skull. Next, mice were placed prone on an in-house designed stereotaxic instrument and the skull was secured by ear bars. To collect CSF, a midsagittal incision of the skin was made posterior to the occipital crest. The subcutaneous tissue and occipital muscles were carefully removed. A sterile syringe fixed to the stereotaxic instrument was then carefully advanced towards the *cisterna magna* by a fraction of about one millimeter and CSF was slowly aspirated. This method typically allowed collection of 3-5 µl of CSF without visible signs of contaminating blood. Immediately after extraction, the CSF samples were flash-frozen in liquid nitrogen and stored at -80°C until further use. Directly after CSF extraction, whole brains were dissected from each mouse, washed once in ice-cold PBS and divided in halves by sagittal dissection on ice. One cerebral hemisphere was further dissected at 4°C in order to obtain the cerebellum, hippocampus, striatum and the cortex regions. Dissected brain regions were immediately flash-frozen in liquid nitrogen and stored at -80°C until further use.

MS Sample Preparation

Shortly before use, CSF was thawed on ice and centrifuged at 16,000 g at 4°C for 15 min to remove any potential contaminations. Clarified CSF was mixed with 40 µl denaturation buffer (6 M urea, 2 M thiourea, 10 mM Hepes pH 8.0) for subsequent in-solution digestion. Dissected brain regions were thawed on ice, placed in FastPrep-24 tubes filled with LysingMatrix D (MP Biomedicals, Eschwege, Germany) and mixed with RIPA buffer supplemented with protease inhibitors (Roche, Mannheim, Germany) and Benzonase (Sigma-Aldrich, Germany). Lysis was achieved by running six times for one min at 4.0 m/s, whereas samples were chilled on ice after each run for one min. Next, the lysed brain regions were separated into pellet and supernatant fraction by centrifugation at 16,000 g at 4°C for 15 min. Soluble proteins in the supernatant were quantified using a tryptophan fluorescence emission assay (Kulak et al., 2014). After protein concentration estimation, 200 µg protein lysate was precipitated for two hours at -20°C with ice-cold acetone. Samples were centrifuged at 16,000 g at 4°C for 20 min and the supernatant was discarded. The precipitated proteins were mixed with 80 µl denaturation buffer (6 M urea, 2 M thiourea, 10 mM Hepes pH

8.0) for subsequent in-solution digestion. The insoluble pellet fraction from the initial lysate clarification was boiled with 100 µl 2% SDS for 10 min at 95°C. After centrifugation at 16,000 g at 4°C for 10 min, the supernatant was discarded and the pellet was washed three times in 2% SDS and three times in PBS for 5 min at 1,000 rpm, followed by centrifugation after each step at 16,000 g at 4°C for 10 min. Next, the pellet fraction was incubated with 100 µl 90% formic acid at 37°C and 1,000 rpm for 45 min. Finally, the pellet samples were snap-frozen in liquid nitrogen and lyophilized overnight in a cold-trap centrifugal evaporator. The next morning, the samples were re-solubilized in 50 µl denaturation buffer (6 M urea, 2 M thiourea, 10 mM Hepes pH 8.0) for subsequent in-solution digestion.

For the in-solution digestion, proteins were digested by LysC (1:100 enzyme to protein ratio; Wako Chemicals, Japan) for three hours at 37°C, followed by trypsin (1:100 enzyme to protein ratio; Sigma-Aldrich) overnight at 37°C. All samples were finally desalted on SDB-RPS StageTips (3M, Empore, Neuss, Germany) and eluted as described (Kulak et al., 2014).

MS Data Processing

All data was analyzed using the MaxQuant software package 1.5.1.1 (Cox and Mann, 2008). The false discovery rate (FDR) cut-off was set to 1% for protein and peptide spectrum matches. Peptides were required to have a minimum length of 7 amino acids and a maximum mass of 4600 Da. MaxQuant was used to score fragmentation scans for identification based on a search with an initial allowed mass deviation of the precursor ion of a maximum of 4.5 ppm after time-dependent mass calibration. The allowed fragment mass deviation was 20 ppm. Fragmentation spectra were identified using the UniprotKB *Mus musculus* database (UniProt, 2015), based on the 2014_07 release, combined with 262 common contaminants by the integrated Andromeda search engine (Cox et al., 2011). Enzyme specificity was set as C-terminal to arginine and lysine, also allowing cleavage before proline, and a maximum of two missed cleavages. Carbamidomethylation of cysteine was set as fixed modification and N-terminal protein acetylation as well as methionine oxidation as variable modifications. Both ‘label-free quantification (MaxLFQ)’ with a minimum ratio count of 1 and ‘match between runs’ with standard settings were enabled (Cox et al., 2014). We used cell type- and brain region- resolved brain proteome data (Sharma et al., 2015) as additional library to gain matching peptide identifications (Tyanova et al., 2016a). Protein copy number estimates were calculated

using the iBAQ algorithm (Schwanhausser et al., 2011), in which the sum of all tryptic peptides intensities for each protein is divided by the number of theoretically observable peptides. Copy number ranking sorts values from the highest to the lowest value.

MS Data Analysis and Visualization

Basic data handling, normalization, statistics and annotation enrichment analysis was performed with the Perseus software package (Tyanova et al., 2016b). We filtered for 8,455 protein groups (soluble proteome), 778 proteinGroups (CSF) and 1495 proteinGroups (insoluble proteome) that were quantified with at least two valid values in at least one group of triplicates. CSF data was additionally filtered according to known GO annotations (CC_extracellular space; BP_secretion; BP_body fluid secretion) and an in-house curated human CSF dataset (unpublished). Missing values were imputed with values representing a normal distribution (generated at 1.8 standard deviations of the total intensity distribution, subtracted from the mean, and a width of 0.3 standard deviations). Volcano plots were generated as described (Keilhauer et al., 2015). Differentially expressed proteins were identified by three-way ANOVA test at a permutation-based FDR cutoff of 0.05. Pathway enrichment analysis was performed based on a Fisher exact test with a Benjamini-Hochberg FDR cutoff of 0.02. GOCC, GOBP, GOMF, CORUM, Pfam domains and KEGG pathway annotations were used for the analysis. The algorithm used for annotation matrix testing is based on a two-dimensional version of the nonparametric Mann-Whitney test, with a p-value threshold of 0.005 (Geiger et al., 2012). 1D annotation enrichment score was calculated on the basis of the protein expression fold change between WT and R6/2 sample groups (Cox and Mann, 2012). All sequence analyses of the mouse proteome were performed on the manually curated part of Uniprot (SwissProt) release 2015_03 (UniProt, 2015). For the prediction of coiled coils the tool ‘coils’ (Lupas et al., 1991) was used. The coiled coil probability cutoff was set to 0.8. PolyQ regions were determined by computationally scanning the *M. musculus* proteome for consecutive runs of glutamine of a minimum length of six residues (not allowing for any non-glutamine residues within). Prediction of low complexity regions was performed as described (Wootton and Federhen, 1993) with a minimal length of 35 residues.

PC12 Cell Viability Assays and Biochemical Assays

For the starvation assay, all serum was removed from the beginning of the experiment. Cells were seeded on coverslips in 24-well cell culture plates for both immunofluorescence microscopy studies and viability assays. After 12 h plated cells were transfected with either mCherry plasmid as control, or the different candidate's plasmids and induced 5 h after transfection. All plasmid transfections were performed with Lipofectamine LTX with Plus Reagent (15338100, Thermo Fisher Scientific) according to manufacturer's instructions. For viability studies, 50 µl of the medium from each well and each condition were taken at 60 h post-transfection. The LDH assay was performed according to manufacturer's instructions (Pierce LDH cytotoxicity Assay Kit, Thermo Fisher Scientific) and absorbance was measured at 490 nm. Filter retardation assay was performed using slot-blotting essentially as described (Scherzinger et al., 1997) with primary antibodies against GFP (1:1,000, 3H9, Chromotek). For description of Western blotting, see Supplementary Experimental Procedures.

Immunohistochemistry

Brains of female R6/2 mice and control littermates of different ages were collected after transcardial perfusion with 4% paraformaldehyde in PBS, followed by overnight fixation. Whole brains were then embedded in albumin-gelatin medium (45% albumin, 1.5% gelatin, in 1 M sodium acetate pH 6.5) and sectioned on a vibratome 1000S (Leica). For some stainings, antigen retrieval was performed in 10 mM sodium citrate buffer (10 mM sodium citrate, 0.05% Tween 20, pH 6) at 80°C for 30 min. Floating sections of 50 µm were permeabilized with 0.5% TritonX-100 for 20 min and then blocked for 2 hours with 0.2% BSA, 5% donkey serum, 0.2% lysine, 0.2% glycine in PBS and permeabilized again. Sections were incubated overnight at 4°C with primary antibodies against mHtt (EM48 1:500, MAB5374, Milipore), DARPP-32 (1:500, ab40801, Abcam), PLP1 (1:100, ab28486, Abcam), hnRNPA2B1 (1:100, sc-374053, SantaCruz Biotechnology) in 0.3% TritonX-100, 2% BSA in PBS, and washed three times with PBS. Sections were then incubated with Cy2-conjugated anti-rabbit (1:200, 711-545-152, Jackson ImmunoResearch), Cy3-conjugated anti-mouse (1:200, 715-165-151 Jackson ImmunoResearch) secondary antibodies and/or NeuroTrace 640/660 Nissl Stain (1:1000, N21483, Thermo Fisher Scientific). Nuclei were counterstained with 4', 6-diamidino-2-phenylindole (DAPI, Sigma-Aldrich) and sections were mounted with Mowiol (in-house preparation).

PC12 cells were fixed 60 h post-transfection in 4% paraformaldehyde in PBS for 15 min, then permeabilized in 0.1% TritonX-100 for 5 min and washed three times in PBS. Blocking was performed for 30 min as described above. Coverslips were incubated for 1 h at room temperature with primary antibodies: anti-myc (1:250, 2278, Cell Signaling), anti-Flag (1:500, F7425, Sigma-Aldrich) and anti-HA (1:500, 11867423001, Roche) followed by Cy3-conjugated anti-rabbit secondary antibody (1:200, 711-165-152, Jackson ImmunoResearch). Nuclei were counterstained with DAPI (Sigma-Aldrich) and coverslips were mounted with ProLong Gold antifade reagent (P36930, Life Technologies). Sections and coverslips were examined at a Confocal TCS SP8 microscope (Leica). Images were taken using a 40x objective.

Aggregate Quantification in Cells and Tissues

Aggregates were quantified using an in-house macro on the freeware ImageJ version 1.49i (NIH). For R6/2 brain sections, aggregates were counted in 20 different confocal stacks in each brain region, in a total of 3 independent experiments. For PC12 cells, aggregates were analyzed in 20 different fields of view for each candidate, in a total of 3 independent experiments. For the quantification of cells with hnRNPA2B1 nuclear accumulation, images were analyzed with an in-house developed pipeline for CellProfiler™, in 20 different fields of view for each mouse brain, in a total of 3 R6/2 mouse brains. The fluorescence intensity analysis was performed with ImageJ. All quantifications were performed in a blinded setting.

Western Blotting

Dissected brain regions were homogenized in lysis buffer containing 50 mM Tris-HCl, pH 7.5, 150 mM NaCl, 1% Triton X-100, 2mM EDTA and protease inhibitor tablet (Roche). For SDS-PAGE, 100 µg of proteins were separated in a 10% gradient gel and transferred to a PVDF membrane. The membrane was blotted with the following primary antibodies: hnRNPA2B1 (1:500, sc-374053, Santa Cruz Biotechnology, Inc.), HSP90 (1:1000, 4877, New England Biolabs GmbH), KIF3B (1:500, sc-514165, Santa Cruz Biotechnology, Inc.), β-Actin (1:2500, A5316, Sigma-Aldrich). After incubation with HRP-conjugated secondary antibodies, the bound antibodies were visualized by chemiluminescence. The intensity of the bands was quantified by Image J software.

Tables

Table S1. Protein expression data for total proteome measurements. Related to Figure 2. Log_2 MaxLFQ intensities and iBAQ copy numbers of proteins detected in the total soluble proteome of R6/2 and WT mice for all brain regions and across time.

Table S2. Protein expression data for CSF measurements. Related to Figure 4. Log_2 MaxLFQ intensities and iBAQ copy numbers of proteins detected in the cerebrospinal fluid of R6/2 and WT mice for all brain regions and across time.

Table S3. Protein expression data of WT and R6/2 mice for insoluble proteome measurements. Related to Figure 5. Log_2 MaxLFQ intensities and iBAQ values of proteins detected in the total insoluble proteome of R6/2 and WT mice for all brain regions and across time. Sequence motives with corresponding lengths and iBAQ ratios for soluble/insoluble iBAQ values are annotated. T-test difference and $-log_{10}$ p-values for R6/2 against WT comparisons were calculated in Perseus.

Table S4. Information about follow-up candidates. Related to Figure 6. Details of function, localization and known linkage to neurodegenerative diseases are indicated.

Supplemental References

Cox, J., Hein, M.Y., Luber, C.A., Paron, I., Nagaraj, N., and Mann, M. (2014). Accurate proteome-wide label-free quantification by delayed normalization and maximal peptide ratio extraction, termed MaxLFQ. Molecular & cellular proteomics : MCP *13*, 2513-2526.

Cox, J., and Mann, M. (2008). MaxQuant enables high peptide identification rates, individualized p.p.b.-range mass accuracies and proteome-wide protein quantification. Nature biotechnology *26*, 1367-1372.

Cox, J., and Mann, M. (2012). 1D and 2D annotation enrichment: a statistical method integrating quantitative proteomics with complementary high-throughput data. BMC bioinformatics *13 Suppl 16*, S12.

Cox, J., Neuhauser, N., Michalski, A., Scheltema, R.A., Olsen, J.V., and Mann, M. (2011). Andromeda: a peptide search engine integrated into the MaxQuant environment. Journal of proteome research *10*, 1794-1805.

Garcia-Cardena, G., Fan, R., Shah, V., Sorrentino, R., Cirino, G., Papapetropoulos, A., and Sessa, W.C. (1998). Dynamic activation of endothelial nitric oxide synthase by Hsp90. Nature *392*, 821-824.

Geiger, T., Wehner, A., Schaab, C., Cox, J., and Mann, M. (2012). Comparative proteomic analysis of eleven common cell lines reveals ubiquitous but varying expression of most proteins. Molecular & cellular proteomics : MCP *11*, M111 014050.

Keilhauer, E.C., Hein, M.Y., and Mann, M. (2015). Accurate protein complex retrieval by affinity enrichment mass spectrometry (AE-MS) rather than affinity purification mass spectrometry (AP-MS). Molecular & cellular proteomics : MCP *14*, 120-135.

Kulak, N.A., Pichler, G., Paron, I., Nagaraj, N., and Mann, M. (2014). Minimal, encapsulated proteomic-sample processing applied to copy-number estimation in eukaryotic cells. Nature methods *11*, 319-324.

Lupas, A., Van Dyke, M., and Stock, J. (1991). Predicting coiled coils from protein sequences. Science *252*, 1162-1164.

Manchanda, P.K., Jones, G.N., Lee, A.A., Pringle, D.R., Zhang, M., Yu, L., La Perle, K.M., and Kirschner, L.S. (2013). Rac1 is required for Prkar1a-mediated Nf2 suppression in Schwann cell tumors. Oncogene *32*, 3491-3499.

Scherzinger, E., Lurz, R., Turmaine, M., Mangiarini, L., Hollenbach, B., Hasenbank, R., Bates, G.P., Davies, S.W., Lehrach, H., and Wanker, E.E. (1997). Huntingtin-encoded polyglutamine expansions form amyloid-like protein aggregates in vitro and in vivo. Cell *90*, 549-558.

Schwanhausser, B., Busse, D., Li, N., Dittmar, G., Schuchhardt, J., Wolf, J., Chen, W., and Selbach, M. (2011). Global quantification of mammalian gene expression control. Nature *473*, 337-342.

Sharma, K., Schmitt, S., Bergner, C.G., Tyanova, S., Kannaiyan, N., Manrique-Hoyos, N., Kongi, K., Cantuti, L., Hanisch, U.K., Philips, M.A*., et al.* (2015). Cell type- and brain region-resolved mouse brain proteome. Nat Neurosci.

Tyanova, S., Temu, T., and Cox, J. (2016a). The MaxQuant computational platform for mass spectrometry-based shotgun proteomics. Nature protocols *11*, 2301-2319.

Tyanova, S., Temu, T., Sinitcyn, P., Carlson, A., Hein, M.Y., Geiger, T., Mann, M., and Cox, J. (2016b). The Perseus computational platform for comprehensive analysis of (prote)omics data. Nature methods.

UniProt, C. (2015). UniProt: a hub for protein information. Nucleic acids research *43*, D204-212.

Wootton, J., and Federhen, S. (1993). Statistics of local complexity in amino acid sequences and sequence databases. Computers & chemistry *17*, 149-163.

Zhang, X., Davis, J.Q., Carpenter, S., and Bennett, V. (1998). Structural requirements for association of neurofascin with ankyrin. The Journal of biological chemistry *273*, 30785-30794.